

Oxidation-induced Lattice Distortion at 4H-SiC (0001) Surface Characterized by Surface Sensitive In-plane X-ray Diffractometry

Adhi Dwi Hatmanto and Koji Kita

Department of Materials Engineering, The University of Tokyo

7-3-1 Hongo, Bunkyo-ku, Tokyo, 113-8656, Japan

Phone: +81-3-5841-7164 E-mail: hatmanto@scio.t.u-tokyo.ac.jp

Abstract

Oxidation-induced lattice distortions at 4H-SiC (0001) surface were investigated by using in-plane X-ray diffractometry. The lattice distortion up to ~0.4% was observed by increasing oxide thickness to 44 nm, which was not recovered even after removing all SiO₂ layer. Ar gas annealing could partially reduce the lattice distortion, indicating the strain relaxation. A significantly lower lattice distortion at 4H-SiC surface was clearly observed for wet oxidation compared to dry oxidation.

1. Introduction

4H-SiC is a promising material for high temperature and high frequency power devices due to its wide band gap, high breakdown field, high thermal conductivity, and the formation of SiO₂ by thermal oxidation [1, 2]. But, the existence of electrically active defects at the SiO₂/SiC interface significantly deteriorates the performance of 4H-SiC MOSFET. As reported in theoretical study [3], the formation of interface defects may partly origin from oxidation-induced local strains on SiC surface, in accordance with a change in electrical structure of SiC. Recently oxidation-induced macroscopic distortion of the SiC wafer surface was also studied [4]. In this paper, we systematically investigated the lattice distortions at 4H-SiC surface region after various oxidation processes directly from the changes in interplanar spacing of 4H-SiC crystal.

2. Experimental Methods

Samples were prepared by performing several kinds of thermal oxidation processes of n-type 4H-SiC (0001), including dry oxidation in 100% oxygen (O₂) at 1300 °C for various oxidation times in a ramp-heating furnace and wet oxidation in 90% H₂O: 10% O₂ at 1100 °C for 2 hours in a tube furnace. Another set of samples was prepared by performing dry oxidation process, then the thermally grown SiO₂ layer were gradually removed by using buffered hydrogen fluoride (BHF) solution for various etching times. Ar gas annealing was also performed at 1150 and 1300 °C for 10 minutes. All samples were characterized by using in-plane x-ray diffractometry (in-plane XRD) to determine the interspacing of lattice planes perpendicular to the surface normal of the 4H-SiC. The shallow incident angles from 0.23 to 1.25 degree were employed to limit the x-ray penetration depth. $2\theta\chi/\phi$ scanning was used, where $2\theta\chi$ and ϕ attributed to the angles of the detector and the sample rotation, parallel

to the 4H-SiC surface normal, respectively. Note that the x-ray penetration depth dramatically changes from several to hundreds of nanometer by increasing the x-ray incident angle. By determining the diffraction patterns at various incident angles, the oxidation-induced lattice distortion in 4H-SiC at various depths was investigated.

3. Results and Discussion

In-plane and out-of-plane XRD patterns of 4H-SiC (0001) substrate before oxidation process were shown in Fig. 1(a). The only one high intensity peak was observed at $2\theta\chi/\phi$ around 33.36°. This peak is attributed to the (10-10) m-face in 4H-SiC crystal, which is perpendicular to (0001) lattice plane. Fig. 1(b) and (c) showed the effects of incident angle on the peak position for the samples before and after oxidation, respectively. As shown in Fig. 1(b), no significant peak position shift was observed, indicating that $d_{(10-10)}$ of 4H-SiC before oxidation was almost constant in various depth. This position is quite close to the one expected from literature for bulk crystal [5], but seems slightly lower possibly due to a little strain on the as-received wafer. On the other hand, peak position of oxidized 4H-SiC sample shifted to the lower angle for small incident angle but gradually shifted back by increasing the incident angle, indicating the difference of $d_{(10-10)}$ between the shallow and deep region.

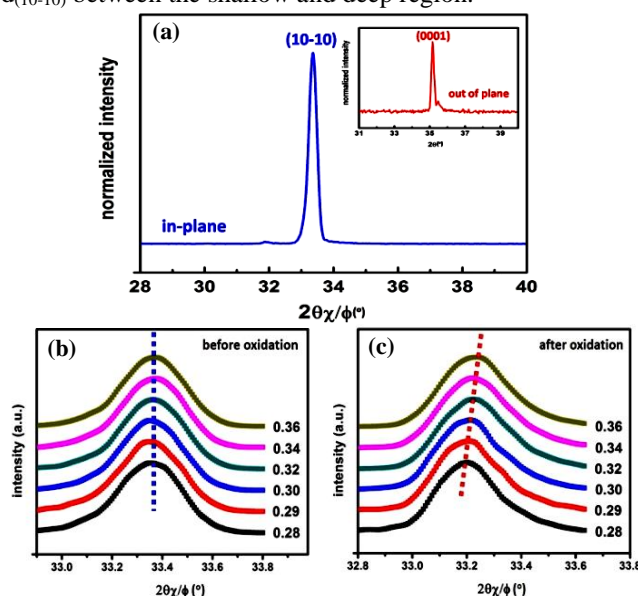


Fig. 1 (a) in-plane and out of plane XRD pattern of 4H-SiC (0001) wafer and the effect of incident angle on the peak position (b) before and (c) after oxidation.

SiO₂ layer with thickness of 12, 29, and 44 nm, were thermally grown by performing dry oxidation for different time. **Fig. 2(a)** shows the relationship between $2\theta\chi/\phi$ peak angle and the incident angle for various SiO₂ thicknesses. At the same incident angle, the peak position of SiO₂/SiC sample prepared in longer oxidation time was observed at lower degree. It describes the changes in $d_{(10-10)}$ of 4H-SiC at various penetration depth, as shown in **Fig. 2(b)**. Penetration depth of x-ray into 4H-SiC was determined by using similar method as reported in Ref. [6] (1.54 Å x-ray wavelength and 3.22 g/cm³ density of SiC were assumed to calculate the penetration depth). According to **Fig. 2(b)**, at the same penetration depth, higher $d_{(10-10)}$ was observed from SiO₂/SiC samples with thicker oxide layer, which indicated that longer oxidation time induced higher lattice distortion. The maximum increase of $d_{(10-10)}$ up to 0.4% was observed at the surface of the 44 nm sample.

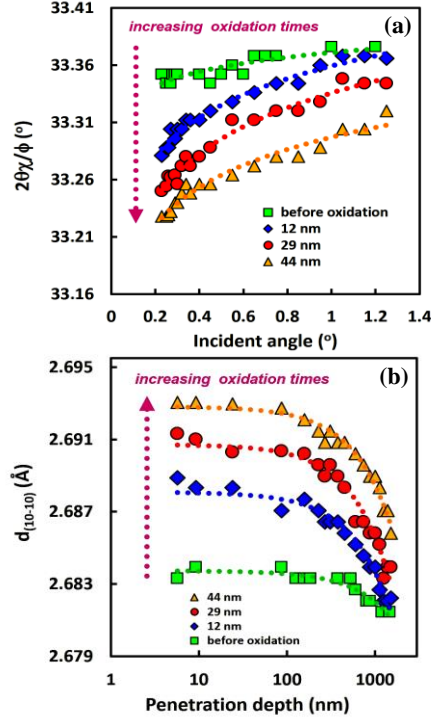
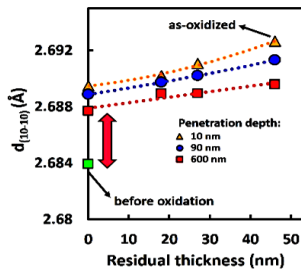


Fig. 2 Relationships between (a) in-plane XRD peak position and incident angle, and (b) $d_{(10-10)}$ interplanar spacing and x-ray penetration depth, which was deduced from (a), for the samples before and after the oxidation with different SiO₂ thickness (12, 29, and 44 nm).

Fig. 3 Relationship between residual SiO₂ thickness and $d_{(10-10)}$ at different penetration depth.



Next, the SiO₂ layer was gradually removed from 46 nm (as-oxidized) to 0 nm (totally removed) by chemical etching. **Fig. 3** represents the relationship between residual thicknesses of SiO₂ and $d_{(10-10)}$ of SiC at penetration depth around 10, 90, and 600 nm. Removing SiO₂ layer gradually

reduces the lattice distortion, but it was insignificant. The most important point is that even SiO₂ layer was totally removed, more than half of the lattice distortion still exists.

The effect of Ar annealing on the lattice of SiC after oxidation process was also studied. We performed Ar annealing at 1150 and 1300 °C for SiC samples after dry oxidation and BHF etching process. As clearly shown in **Fig. 4(a)**, the Ar annealing process could partially reduce the lattice distortion of SiC. The effect of annealing process on the lattice distortion recovery was faster at temperature of 1300 compared to 1150 °C.

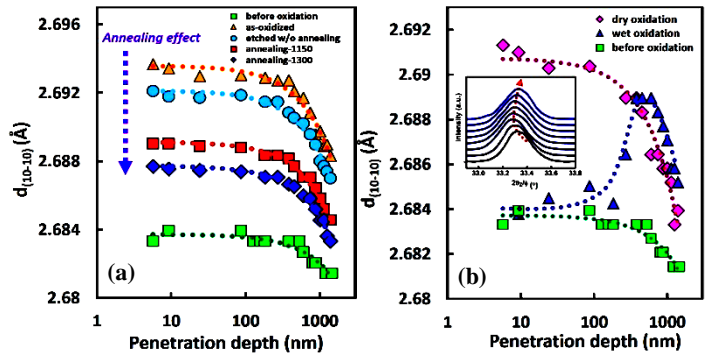


Fig. 4 Effects of (a) Ar annealing and (b) dry vs wet oxidation on x-ray penetration depth dependence of $d_{(10-10)}$.

Fig. 4(b) depicts the comparison of $d_{(10-10)}$ of the samples prepared by dry and wet oxidation processes. It clearly shows the difference between $d_{(10-10)}$ of 4H-SiC prepared by dry and wet oxidation processes, especially on the surface region. This trend of $d_{(10-10)}$ in wet oxidation sample was also clarified from the inset, where the peak position was firstly shifted to the lower degree, and then shifted back to the higher degree by increasing the incident angle. This result indicated that wet oxidation process resulting lower strain at the 4H-SiC surface due to lower lattice distortion. This will be correlated with the observation that a lower strain in SiO₂ was also observed for wet oxidation.

4. Conclusions

The oxidation-induced lattice distortion at the 4H-SiC surface region was clarified by in-plane XRD measurements. It was strongly affected by oxidation processes (dry or wet), while the partial recovery could be done by Ar annealing, but not by removing the oxide layer. Our results reveal that oxidation processes should have a significant impact to the quality of the 4H-SiC surface.

Acknowledgements

This work was partially supported by CSTI, Cross-ministerial Strategic Innovation Promotion Program, "Next-generation power electronics" (funding agency: NEDO), and by JSPS KAKENHI.

References

- [1] K. Fukuda, S. Suzuki, T. Tanaka, Appl. Phys. Lett. **76**(2000)12.
- [2] Z. Qiaozhi and W. Dejun, J. Semicond. **35**(2014)2.
- [3] K. Shiraishi *et al.*, IEDM. **14**(2014)21.
- [4] X. Li *et al.*, Appl. Phys. Lett. **110**(2017).
- [5] M. Stockmeier *et al.*, Appl. Phys. Lett. **105**(2009).
- [6] L. L. Fan *et al.*, J. Alloys and Comp. **678**(2016).